THE JOURNAL OF BIOLOGICAL CHEMISTRY VOL. 289, NO. 10, pp. 7190–7199, March 7, 2014

Cryo-electron Microscopic Structure of SecA Protein Bound to the 70S Ribosome*[S]

Received for publication, July 30, 2013, and in revised form, January 15, 2014 Published, JBC Papers in Press, January 17, 2014, DOI 10.1074/jbc.M113.506634

Rajkumar Singh[‡], Christian Kraft[‡], Rahul Jaiswal[§], Kushal Sejwal[‡], Vikram Babu Kasaragod[‡], Jochen Kuper[‡], Jörg Bürger[¶‖], Thorsten Mielke[¶‖], Joen Luirink[**], and Shashi Bhushan[‡§1]

From the [‡]Rudolf Virchow Center/DFG Research Center for Experimental Biomedicine, University of Würzburg, Josef Schneider Str. 2, 97078 Würzburg, Germany, the [§]Division of Structural Biology and Biochemistry, School of Biological Sciences, Nanyang Technological University, Singapore 637551, the [¶]UltraStrukturNetzwerk, Max Planck Institute for Molecular Genetics, Ihnestr. 73, 14195 Berlin, Germany, the [‖]Institut für Medizinische Physik und Biophysik, Charité, Ziegelstrasse 5–8, 10117 Berlin, Germany, and the [**]Department of Molecular Microbiology, Institute of Molecular Cell Biology, Vrije Universiteit, 1081 HV Amsterdam, The Netherlands

Background: SecA targets preproteins to the protein-conducting channel in bacteria.
Results: Both the single and double copies of SecA bind to the 70S ribosome.
Conclusion: Two copies of SecA completely surround the polypeptide tunnel exit.
Significance: The structures suggest a function of the dimeric form of SecA on the ribosome.

SecA is an ATP-dependent molecular motor pumping secretory and outer membrane proteins across the cytoplasmic membrane in bacteria. SecA associates with the protein-conducting channel, the heterotrimeric SecYEG complex, in a so-called posttranslational manner. A recent study further showed binding of a monomeric state of SecA to the ribosome. However, the true oligomeric state of SecA remains controversial because SecA can also form functional dimers, and high-resolution crystal structures exist for both the monomer and the dimer. Here we present the cryo-electron microscopy structures of *Escherichia coli* SecA bound to the ribosome. We show that not only a monomeric SecA binds to the ribosome but also that two copies of SecA can be observed that form an elongated dimer. Two copies of SecA completely surround the tunnel exit, providing a unique environment to the nascent polypeptides emerging from the ribosome. We identified the N-terminal helix of SecA required for a stable association with the ribosome. The structures indicate a possible function of the dimeric form of SecA at the ribosome.

Protein translocation across the cytoplasmic membrane and insertion into the membrane are mediated by a universally conserved membrane-bound heterotrimeric Sec translocase, the protein conducting channel. Sec translocase in bacteria is called the SecYEG complex, in which subunit Y forms a translocation channel (1–3). The SecYEG complex can be directly associated with the translating ribosome in a cotranslational manner or with SecA in a posttranslational manner (1, 2). SecA is an essential cytoplasmic protein in bacteria that, together with another partner, SecB, which is not essential, targets preproteins to the SecYEG translocon (4). The majority of substrates for SecA-dependent protein translocation are secretory periplasmic and outer membrane proteins with less pronounced hydrophobic signal sequences than the signal recognition particle (SRP)-dependent[2] substrates (1, 2). SecA is a multidomain protein consisting of two nucleotide-binding domains (NBD1 and NBD2), two helical scaffold domains (HSD-I and HSD-II), a polypeptide cross-linking domain (PPXD), and a helical wing domain. ATP binds at the interface of NBD1 and NBD2 (1). Crystal structures of SecA from different species vary in the position of the PPXD relative to the helical wing domain. The PPXD is either packed against the helical wing domain (5–7) or shifted away from it toward NBD2 (8, 9). The cleft between the PPXD and NBD2 is referred to as the clamp, and, depending on the position of the PPXD, it can be in an open (5), partially open (8), or closed form (10). The PPXD has been proposed to interact with preproteins (11–14).

Purified SecA exists in an equilibrium between a monomeric and dimeric form with an estimated dissociation constant, K_d, of ~1 nM, as determined with the fluorescence cross-correlation spectroscopy method (15). Artificially covalently linked dimeric SecA is functional in protein translocation (3, 16–20). Dimeric SecA dissociates into monomers in the presence of anionic phospholipids (21, 22), and signal peptides have been shown to either dissociate the dimeric form (22, 23) or promote oligomerization (21). Several *in vitro* translocation studies have also indicated that SecA functions as a dimer (16, 19, 24). Attempts to generate a stable monomer by truncation and site-specific mutagenesis were not successful because they resulted

* This work was supported by the Deutsche Forschungsgemeinschaft (Forschungszentrum, Rudolf-Virchow-Zentrum), by the School of Biological Sciences, Nanyang Technological University, Singapore (to S. B.), and by Grant SFB740, Project Z1 from the Deutsche Forschungsgemeinschaft (to T. M.).

[S] This article contains supplemental Figs. S1 and S2.

The cryo-electron microscopic maps of the single ([1]SecA) and double copies ([1]SecA) of SecA bound to the 70S ribosomes have been deposited in the 3D-EM database under accession numbers EMD-2564 and EMD-2565, respectively.

[1] To whom correspondence should be addressed: Div. of Structural Biology and Biochemistry, School of Biological Sciences, Nanyang Technological University, Singapore. Tel.: 65-6592-3673; Fax: 65-6791-3856; E-mail: sbhushan@ntu.edu.sg.

[2] The abbreviations used are: SRP, signal recognition particle; NBD, nucleotide-binding domain; PPXD, polypeptide cross-linking domain; DDM, *n*-dodecyl-β-maltoside; TF, trigger factor.

in severe loss of SecA activity, further supporting the view that the dimeric form is functional (22, 25, 26). Although it is accepted that SecA is dimeric in the cytosol and that high-resolution structures exist for both the monomer and the dimer (5–10), the inability to define the exact role for the second copy in the dimer strongly favors the view that the monomeric form is functional. However, despite major research, the true oligomeric state of SecA remains highly controversial (18). This is further complicated by the different models suggesting association of both the monomeric and dimeric forms of SecA to the SecYEG translocon (27–30), although the structure of the SecA-SecYEG complex suggests a 1:1 interaction (10). The structure of the SecA-SecYEG complex was a major achievement, but it failed to explain the observed interactions between SecA and SecYEG during translocation (10, 31–33). SecA alone has also been suggested to promote protein translocation independently of SecYEG (34–36).

SecA has been shown to interact with translating ribosomes (37), and, recently, Huber *et al.* (38) suggested that the monomeric form of SecA binds to the ribosomes through L23 protein on the polypeptide tunnel exit.

Here we determined the cryo-electron microscopy structures (cryo-EM) of both the single and double copies of SecA bound to the 70S ribosome at 10.3 Å and 8.8 Å resolution, respectively. We identified two SecA-binding sites at the tunnel exit of the ribosome that display different affinities for the two SecA molecules. We found that the N-terminal helix of SecA is required for stable association with the ribosome.

EXPERIMENTAL PROCEDURES

Purification of 70S Ribosomes—Ribosomes were purified using a standard sucrose gradient preparation (39). In brief, 2 liters of *Escherichia coli* cells were grown to 0.8 A_{600} in LB medium at 37 °C in an incubator shaker. Cells were harvested and lysed in lysis buffer (40 mM Hepes (pH 7.6), 500 mM potassium acetate, 25 mM magnesium acetate, 2 mM 2-mercaptoethanol, 0.1% protease inhibitor pill/ml, and 250 mM sucrose) using a cell disruptor. The cleared lysate was applied to a sucrose cushion (750 mM sucrose in lysis buffer), and ribosomes were pelleted by ultracentrifugation in a Beckmann TLA 100.4 rotor at 42,000 rpm for 2 h 30 min (4 °C). The ribosome pellet was dissolved in lysis buffer. Crude ribosomes were further purified using a 10 ml 10–40% sucrose gradient in lysis buffer. Gradients were centrifuged in a Beckmann SW40-Ti rotor at 30,000 rpm for 4 h (4 °C), and 0.5 ml fractions were collected using a gradient station (BioComp Instruments, Canada). 70S fractions were pooled and concentrated by ultracentrifugation. The final pellet of 70S ribosome was dissolved in ribosome buffer (40 mM Hepes (pH 7.6), 50 mM potassium acetate, 25 mM magnesium acetate, 5 mM DTT, 0.1% protease inhibitor pill/ml, 0.1 units/ml RNAsin, and 125 mM sucrose).

Purification of SecA—An N-terminally His-tagged *E. coli* construct was obtained from "the National BioResource Project, National Institute of Genetics, Japan: *E. coli*" (40). SecA was overexpressed in *E. coli* BL21 (DE3) cells and purified using a standard nickel affinity purification method. Briefly, 6 liters of bacterial culture was induced with 1 mM isopropyl 1-thio-β-D-galactopyranoside and grown for 4 h at 37 °C. The cleared lysate in SecA buffer (50 mM Hepes (pH 7.6), 300 mM NaCl, 0.1% protease inhibitor pill/ml, and 10 mM imidazole) was applied to a nickel-nitrilotriacetic acid resin, and bound proteins were eluted with 250 mM imidazole in SecA buffer. Imidazole was removed by dialysis overnight against SecA binding buffer (50 mM Hepes (pH 7.6), 100 mM potassium acetate, 5 mM magnesium acetate, and 0.1% protease inhibitor pill/ml) at 4 °C. Purified SecA was concentrated to 2.6 mg/ml and stored at −20 °C.

SecA residues 2–38 were removed in the ΔN38 SecA construct using full-length SecA as a template in the PCR with the following primers: DelN-SecA, ATCTTTATTTTCAGGGCGCCATGTCCGACGAAGAACTGAAAGGG (forward) and GTGCGGCCGCAAGCTTGTCGACTTATTGCAGGCGGCCATGGC (reverse). The purified PCR product was cloned in a pBADM11 vector (EMBL Heidelberg) containing an N-terminal His tag using ligation-independent cloning. ΔN38 SecA was transformed into BL21 (DE3) cells. 6 liters of bacterial culture was induced with 0.05% arabinose and grown overnight at 20 °C in an incubator shaker. His-tagged ΔN38 SecA protein was purified using the same procedure as for full-length SecA. Full-length SecA cDNA was cloned in a pLATE51 vector (Thermo Scientific) with an enterokinase site in between the His tag and SecA. Briefly, full-length SecA was amplified with lic-seca-EK (GGTGATGATGATGACAAGATGCTAATCAAATTGTTAACTAAAGTTTTCG, forward) and lic-seca (GGAGATGGGAAGTCATTATTGCAGGCGGCCATGGCAT, reverse) primers using full-length SecA as a template in the PCR. The purified PCR product was cloned into the pLATE51 vector using ligation-independent cloning. The His-tagged protein with the enterokinase site was purified as above. After purification, the His tag was cleaved off with enterokinase (New England Biolabs) according to the manual of the supplier. Lysine residues at positions 625 and 633 in full-length wild-type SecA (wtSecApLate51) were substituted by alanine using site-directed mutagenesis (New England Biolab) with the following primers: SecAK625A, ATTGAACACCCGTGGGTGACTGCAGCGATTGCCAACGCCCAGCGT (forward) and ACGCTGGGCGTTGGCAATCGCTGCAGTCACCCACGGGTGTTCAAT (reverse); SecAK633A, GCGATTGCCAACGCCCAGCGTGCAGTTGAAAGCCGTAACTTCGAC (forward) and GTCGAAGTTACGGCTTTCAACTGCACGCTGGGCGTTGGCAATCGC (reverse).

Ribosomal Cosedimentation Assay—Purified 70S ribosomes were incubated with the indicated amount of SecA in ribosome buffer at room temperature for 10 min. Reactions were layered on top of a 200 μl sucrose cushion (750 mM sucrose in ribosome buffer). Ribosomes were pelleted in a Beckmann TLA 100 rotor at 45,000 rpm for 2 h 45 min (4 °C). Pelleted ribosomes were analyzed by SDS-PAGE and Coomassie staining. Gels were scanned and quantified using an Odyssey imaging system (Li-COR Biosciences GmbH, Germany).

In Vitro Reconstitution of SecA Ribosome Complexes—Purified *E. coli* 70S ribosomes were reconstituted *in vitro* with purified His-tagged SecA. Briefly, 0.3 μM 70S ribosomes were incubated with 5.5 μM SecA in ribosome buffer and incubated at room temperature for 10 min. Reconstituted samples were immediately applied to grids.

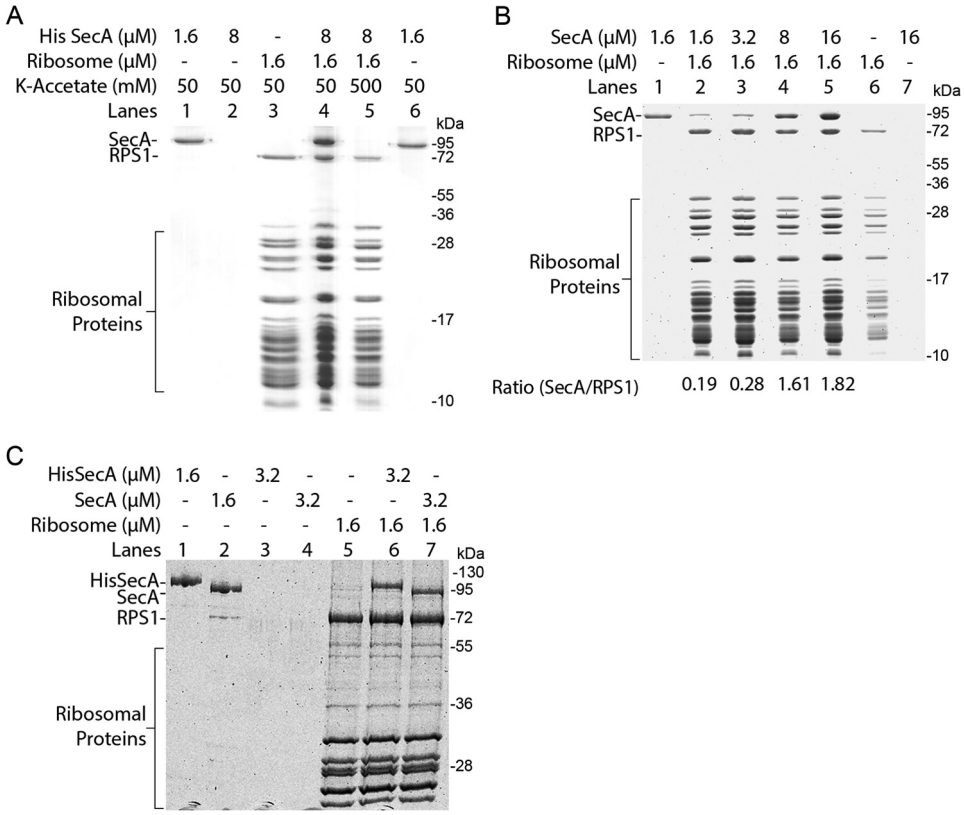

FIGURE 1. **SecA binds to the ribosome.** Binding reactions were pelleted through a sucrose cushion and analyzed on a 15% (*A* and *B*) or 10% (*C*) SDS-PAGE with Coomassie Blue staining. *A*, cosedimentation assay using 1.6 μM purified 70S ribosomes with a 5-fold molar excess of SecA as indicated. SecA specifically cosediments with ribosomes (*lane 4*). No binding was observed at high salt concentrations (*lane 5*), and SecA alone did not sediment (*lane 2*). *Lane 3* shows 1.6 μM of 70S ribosomes pelleted alone. 1.6 μM SecA alone was applied on the gel as a control (*lanes 1* and *6*). *RPS1*, ribosomal protein S1. *B*, about a 5-fold molar excess of SecA is required to saturate ribosome binding. Ribosomes were incubated with increasing concentrations of SecA protein as indicated (*lanes 2–5*). Binding was almost saturated when SecA was present in a 5-fold molar excess (*lane 4*) and increasing the SecA concentration to a 10-fold excess did not significantly increase binding (*lane 5*). SecA alone did not sediment (*lane 7*). *Lane 6* shows 1.6 μM 70S ribosomes pelleted alone. 1.6 μM SecA alone was applied on the gel as a control (*lane 1*). *C*, the His tag does not influence SecA binding to the ribosome. 1.6 μM purified 70S ribosomes were incubated with the indicated amounts of SecA. Both the His-tagged (*lane 6*) and His tag-cleaved SecA (*lane 7*) show comparable binding and equally cosedimented with ribosomes, suggesting no influence of the His tag on ribosome binding. Both the His-tagged and His tag-cleaved SecA alone did not sediment (*lanes 3–4*). *Lane 5* shows 1.6 μM 70S ribosomes pelleted alone. 1.6 μM each of the His-tagged and His tag-cleaved SecA proteins were applied on the gel as a control (*lanes 1* and *2*).

Electron Microscopy, Image Processing, and Modeling—As described previously (41), 3.5 μl of reconstituted samples were applied to 2-nm carbon-coated holey grids (Jena Biosciences). Grids were frozen in liquid ethane using a Vitrobot (FEI) and stored in liquid N_2. Micrographs were recorded under low-dose conditions (25 electrons/Å^2) on a Tecnai G2 Polara TEM operated at 300 kV with 39,000× nominal magnifications at a defocus in the range of 1.0–4.5 μm. Micrographs were scanned on a Heidelberg Primescan D8200 drum scanner, resulting in a pixel size of 1.24 Å on the object scale. The data were analyzed by determination of the contrast transfer function using CTFFIND software (42). The data were further processed with the SPIDER software package (43). After automated particle picking followed by visual inspection, 240,000 particles were selected for density reconstruction. The dataset was sorted (44) using reconstructions of unprogrammed (empty) ribosomes as initial references. The sorting steps were performed at a pixel size of 2.44 Å/pixel, and reference volumes were filtered from 15 Å to 20 Å. Densities for the 30S and 50S subunits were isolated using binary masks. SecA densities were used as such without applying any mask. Low-resolution structures were determined from cryo-EM data recorded at a Tecnai T12 TEM (FEI) equipped with a 4K camera (FEI). About 8000 particles were used for three-dimensional reconstructions. Models were generated with a Swiss homology server and adjusted manually with Coot (45). Initial docking of x-ray structures and cryo-EM maps was performed using Chimera (46). All figures were generated using Chimera (46).

RESULTS AND DISCUSSION

SecA Binds to the 70S Ribosome—We studied SecA interaction with the ribosome by ribosomal cosedimentation assay. 1.6 μM of *E. coli* ribosomes, purified by sucrose density gradient, were incubated with 8 μM purified N-terminally His-tagged *E. coli* SecA. Binding reactions were pelleted through a sucrose cushion, and pellets were analyzed by SDS-PAGE and Coomassie staining. SecA strongly cosedimented when incubated with ribosomes (Fig. 1*A*). Almost no binding of SecA was detected when the salt concentration was increased to 500 mM, thus confirming the salt-sensitive, specific binding of SecA to the ribosome (Fig. 1*A*) proposed recently (38). SecA binding to ribosomes almost showed saturation when a 5-fold molar excess of SecA was used because binding did not increase significantly when the SecA concentration was increased to a 10-fold molar excess (Fig. 1*B*). To rule out that the strong binding of SecA to ribosomes is not due to the His tag present on

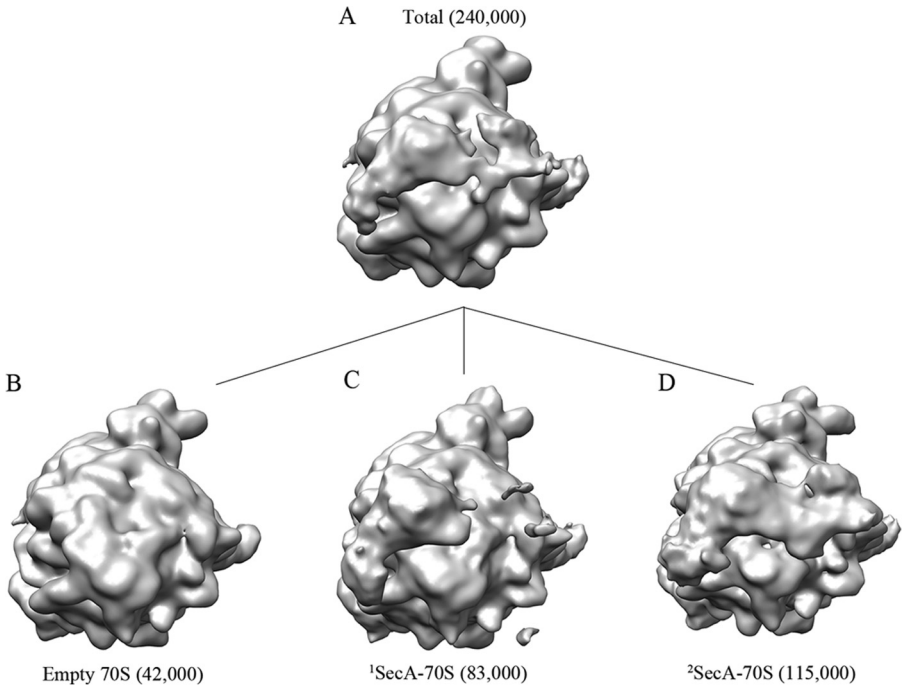

FIGURE 2. ***In silico* sorting of the SecA dataset.** *A*, the total dataset containing ~240,000 particles was sorted *in silico* into three different populations (*B–D*) using a low-resolution, empty 70S ribosome structure as a reference. A sorting analysis resulted in segregation of three distinct 70S populations: with no SecA density visible, empty (~42,000 particles) (*B*), with density for one molecule of SecA, [1]SecA-70S (~83,000 particles) (*C*), and with density visible for two molecules of SecA, [2]SecA-70S (~115,000 particles) (*D*).

SecA, the His tag was cleaved from SecA protein using enterokinase protease as described under "Experimental Procedures." Both the His-tagged and His tag-cleaved SecA showed comparable binding to the ribosome (Fig. 1*C*), ruling out the possible role of the His tag on SecA interaction with the ribosome.

Cryo-EM Reconstruction of SecA Bound to the 70S Ribosome—To obtain a three-dimensional structure of SecA bound to the ribosome, we employed cryo-EM and single particle reconstruction. 70S ribosomes were reconstituted *in vitro* with an excess of His-tagged SecA. Cryo-EM grids were prepared using the reconstituted complex, and micrographs were recorded with a Tecnai G2 Polara (FEI) electron microscope. Data were processed using SPIDER software (43). For simplicity, the terms [1]SecA-70S and [2]SecA-70S are used for the single (monomeric) and double copies (dimeric) of SecA bound to the 70S ribosomes. SecA[1] and SecA[2] are used for the two SecA molecules in the [2]SecA structure, where SecA[1] is equivalent to monomeric SecA in [1]SecA. A preliminary reconstruction showed additional density near the polypeptide tunnel exit (Fig. 2*A*) when compared with the empty ribosome, demonstrating that SecA is indeed bound in the structure. The EM density distribution analysis suggested more density on one side of the tunnel exit (Fig. 2*A*), indicating heterogeneity in the dataset, and, therefore, computational sorting was applied. In brief, two rounds of sorting were applied to segregate different homogenous populations of particles. In the first round, empty particles were sorted out from SecA-bound particles. In the second round, only SecA-bound particles generated from the first round were further sorted into two distinct populations. Empty ribosome with no density at the tunnel exit was used as a counterreference for both rounds to minimize reference-biased sorting. Surprisingly, the sorting analysis resulted in three distinct structures: no density at the tunnel exit site, empty 70S (~17% particles) (Fig. 2*B*); with density at one side of the tunnel exit, corresponding to one copy of SecA-bound 70S ([1]SecA-70S, ~35% particles) (Fig. 2*C*); and with density on both sides of the tunnel exit, two copies of SecA-bound 70S ([2]SecA-70S, ~48% particles) (Fig. 2*D*). SecA-bound 70S subdatasets were refined further, yielding final resolutions of 10.3 and 8.8 Å, respectively (Fig. 3).

Structure of the Single Copy of SecA Interacting with the 70S Ribosome—SecA is a cytoplasmic protein consisting of several domains (Fig. 4*A*). ATP binds at the interface of two nucleotide-binding domains (NBD1 and NBD2). High-resolution crystal structures of SecA from different species exist in three different conformations: the so called open (5) (PDB code 1M74), partially open (8) (PDB code 1TF2), and closed (10) (PDB code 3DIN) states. The main differences between these structures are large-scale movements observed for the entire PPXD. The only SecA crystal structure available from *E. coli* (9) (PDB code 2FSF) is in an open conformation that is not complete. Therefore, homology models of *E. coli* SecA were built using the Swiss homology server (47), provided with an open, a partially open, and closed conformation (PDB codes 1M74, 1TF2, and 3DIN) as templates. Docking of these three structures in the isolated density of [1]SecA showed that SecA bound in this structure is similar to the open conformation (1M74). Thus, the SecA homology model in the open conformation (generated using PDB code 1M74 as a template) was docked into the [1]SecA density using a rigid body followed by manual fitting in Coot (Fig. 4*A* and supplemental Fig. S1). The molecular model of TnaC stalled 50S ribosome (48) (PDB code 2WWQ) fit well in the 50S EM densities of both SecA-bound structures ([1]SecA-

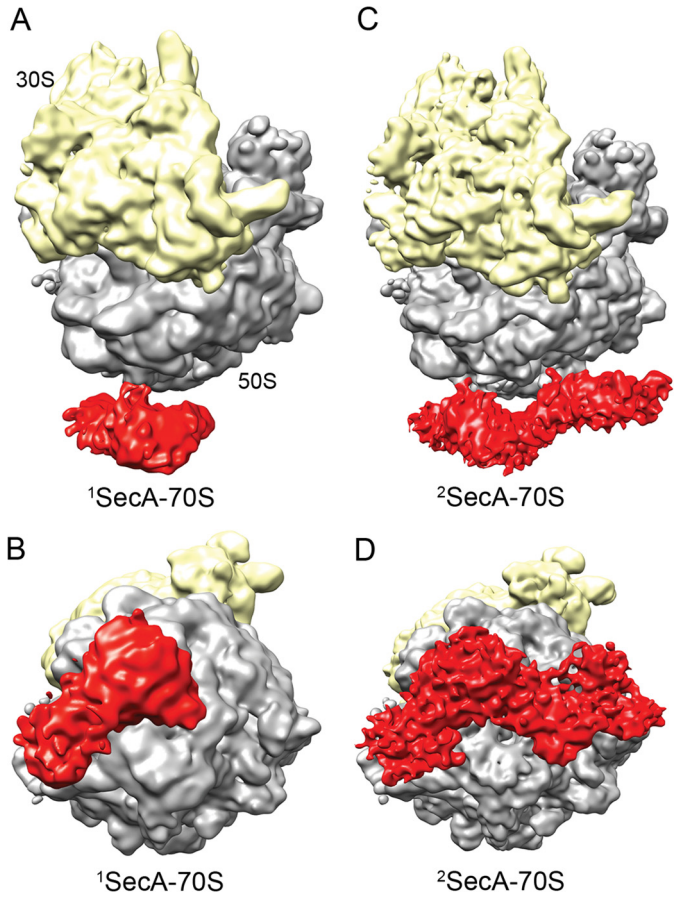

FIGURE 3. **Cryo-EM reconstructions of SecA bound to the 70S ribosome.** *A*, cryo-EM structure of monomeric SecA bound to the 70S ribosome (¹SecA-70S). The 30S small ribosomal subunit and the 50S large subunit are shown in *yellow* and *gray*, respectively. Additional density at the tunnel exit site, shown in *red*, represents monomeric SecA. *B*, the same as *A* but rotated upwards by 90° around the horizontal axis. *C*, cryo-EM structure of two copies of SecA bound to the 70S ribosome (²SecA-70S). The density at the tunnel exit site represents two copies of SecA. The ribosomal subunits and SecA are shown in the same colors as in *A*. *D*, same as *C* but rotated upwards by 90° around the horizontal axis.

and ²SecA-70S) (Fig. 5). The resulting models identified the N terminus of SecA in close vicinity to, and, presumably, interacting with, ribosomal protein L23 at the tunnel exit site (Fig. 4*B*). These results indicate that a single copy of SecA interacts with the ribosome via the proposed universal binding platform provided by L23 protein (49) on the tunnel exit site (Fig. 4*B*). This is also consistent with recent studies indicating cross-linking of SecA to L23 protein (38).

Structure of the Double Copies of SecA Interacting with the 70S Ribosome—The volume of the density corresponding to SecA in the ²SecA structure is roughly twice as large as that of the ¹SecA structure (Fig. 6*A*). Therefore, two copies of the SecA model were fit into the density (Fig. 6*B*). However, in contrast to the ¹SecA structure, the open conformation of SecA did not fit into the two copies of SecA in the ²SecA density. On the contrary, two molecules of SecA in the partially open conformation (generated using PDB code 1TF2 as a template) fit well into the SecA density of the ²SecA structure, suggesting that the PPXD domain adopts a different conformation when SecA is present

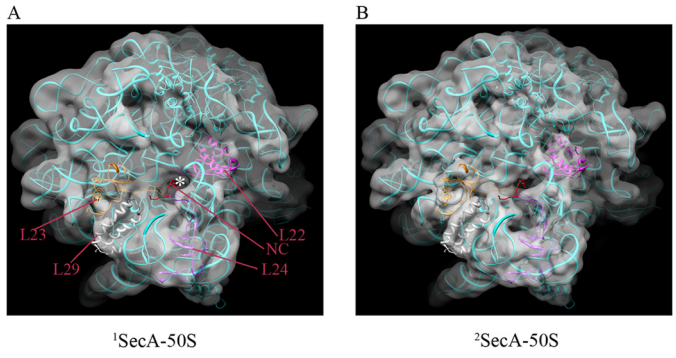

FIGURE 5. **Fitting of the TnaC-stalled 50S model (PDB code 2WWQ) in ¹SecA (*A*) and ²SecA density maps (*B*).** Ribosomal proteins L22, L23, L24, and L29 present at the exit site tunnel are colored in *magenta*, *gray*, *purple*, and *gold/yellow*, respectively. A ribbon model of the TnaC nascent chain in the tunnel is shown in *red*. The tunnel exit is marked with a *white asterisk*.

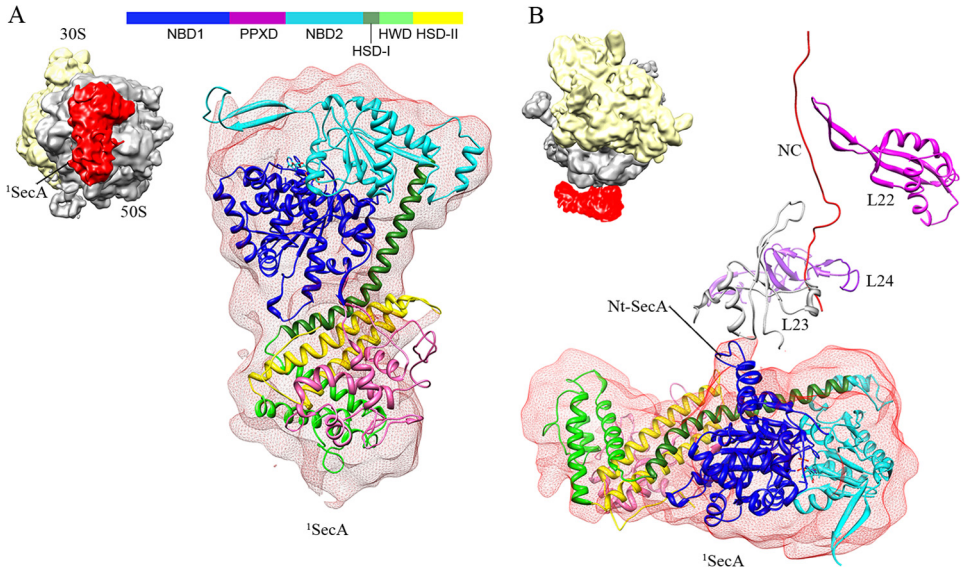

FIGURE 4. **Molecular model of monomeric SecA bound to the 70S ribosome (¹SecA-70S).** *A*, fitting of the *E. coli* SecA model in an open conformation into the density of the SecA monomer. The EM density for SecA is shown in *transparent red*, and the domains of SecA are colored as shown in the schematic. The *small image* shows the orientation of the SecA-ribosome complex. *B*, the N-terminal helix of SecA is in close proximity to the ribosomal protein L23 at the tunnel exit site and, therefore, is presumably involved in interactions with the 70S ribosome. The L22, L23, and L24 proteins are shown in *magenta*, *gray*, and *purple*, respectively. A ribbon model of the TnaC nascent chain (48) (PDB code 2WWQ) is shown in *red* for tunnel orientation. The *small image* shows the orientation of the SecA-ribosome complex.

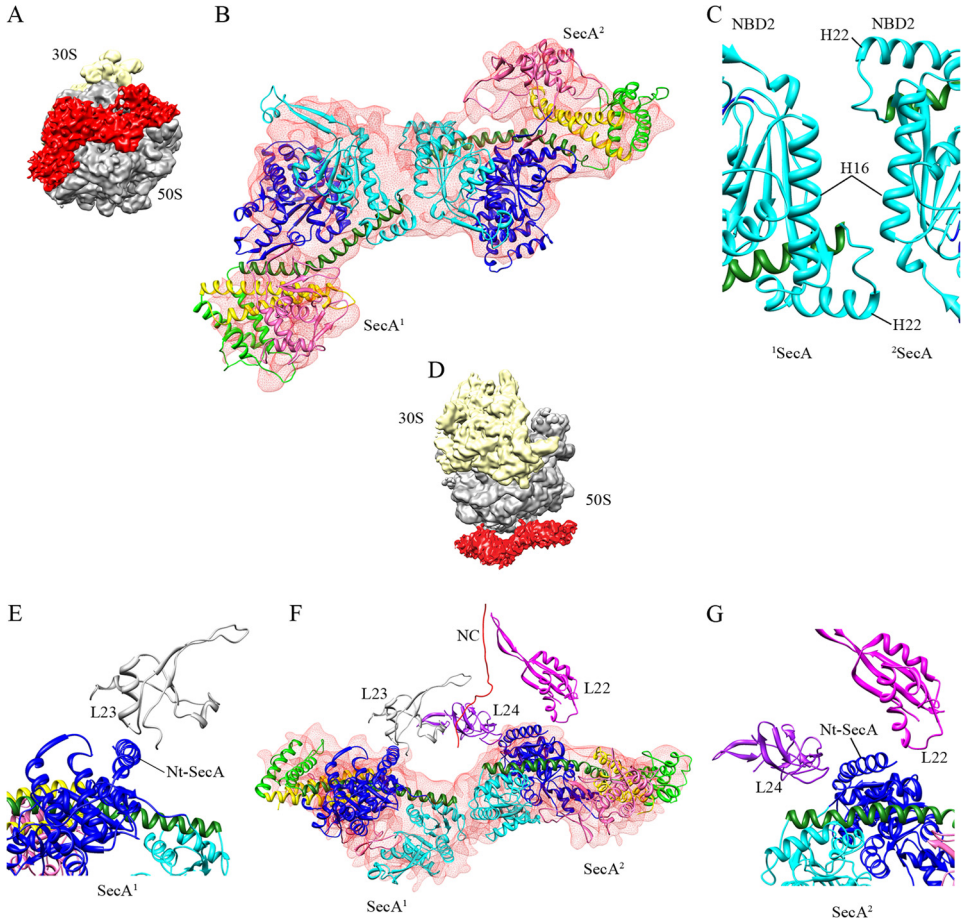

FIGURE 6. **Molecular model of two copies of SecA bound to the 70S ribosome (^{2}SecA-70S).** *A*, the orientation of two molecules of SecA bound to the 70S ribosome. *B*, fitting of the two *E. coli* SecA homology models in partially open conformation into the ^{2}SecA density (shown in *transparent red*). SecA^1 and SecA^2 bind to the 70S ribosome in a back-to-back arrangement, where SecA^2 is rotated ~180° relative to SecA^1 around the vertical axis, producing an approximate 2-fold symmetry. The domains of SecA are colored as in Fig. 4. *C*, close-up view of the interaction between two SecA molecules in the back-to-back arrangement. Helix 22 might interact with helix 16 in both molecules. *D–G*, views of the complex after inward rotation by 90° around the horizontal axis. *D*, the orientation of two molecules of SecA bound to the 70S ribosome. *E–G*, the N-terminal (*Nt*) helix of both SecA molecules is in close proximity to the ribosomal protein L23 for SecA^1 (*E* and *F*) and to L22/L24 for SecA^2 (*F* and *G*). The color scheme is the same as before.

in two copies on the ribosome (Fig. 6). Fitting of the models into the density revealed a back-to-back arrangement of the two SecA molecules when bound to the ribosome (Fig. 6, *B* and *C*), with the two copies being related by an approximate 2-fold symmetry (Fig. 6*B*). Both molecules of SecA only fit into the density when placed in this arrangement. Attempts to fit them in different ways were not successful. The SecA^1 and SecA^2 monomers interact with each other using their NBD2 domains (Fig. 6*C*). Interestingly, as in SecA^1, the SecA^2 molecule also appears to interact with the ribosome, utilizing its N-terminal helix, which is in close proximity to the ribosomal proteins L22 and L24 on the opposite side of the tunnel exit compared with SecA^1 (Fig. 6, *E–G*). This suggests that both SecA molecules in the ^{2}SecA structure bind to the ribosome using their N termini. These findings are also supported by experiments from Huber *et al.* (38), where the authors found that SecA can also weakly cross-link to the L22 protein, although they propose that this interaction is not specific.

The N-terminal Region of SecA Is Required for Stable Interaction with the Ribosome—To address the role of the N-terminal helix in ribosomal interaction in more detail, residues 2–38 were deleted, resulting in a His-tagged ΔN38 SecA construct. The ribosomal cosedimentation assay showed no significant binding of ΔN38 SecA protein to the ribosome (Fig. 7*A*). Additionally, no SecA density was observed when a low-resolution ribosome structure was determined using 70S ribosomes reconstituted with His-tagged ΔN38 SecA (Fig. 7*C*). Purified His-tagged ΔN38 SecA protein was soluble and displayed a similar behavior as full-length SecA when analyzed with circular dichroism spectroscopy (Fig. 7*D*). These results are in conflict with Huber *et al.* (38), who showed that the α-helical linker domain (residues 616–668) of SecA is required for binding to the ribosomes. We repeated the ribosome binding experiments with a SecA variant where lysine 625 and 633 are replaced with alanine (SecA[K625A/K633A]), as used earlier by *Huber et al* (38). The ribosomal cosedimentation assay showed a slight decrease in binding of the SecA[K625A/K633A] protein to the ribosome as compared with wild-type SecA protein (Fig. 7*E*). However, we could not fit the SecA model into the density when this α-helical domain was placed in close vicinity to L23 protein on the ribosome. Upon careful examination of the various crystal structures of SecA available from the PDB, we found that this α-helical linker lies close to the N terminus of

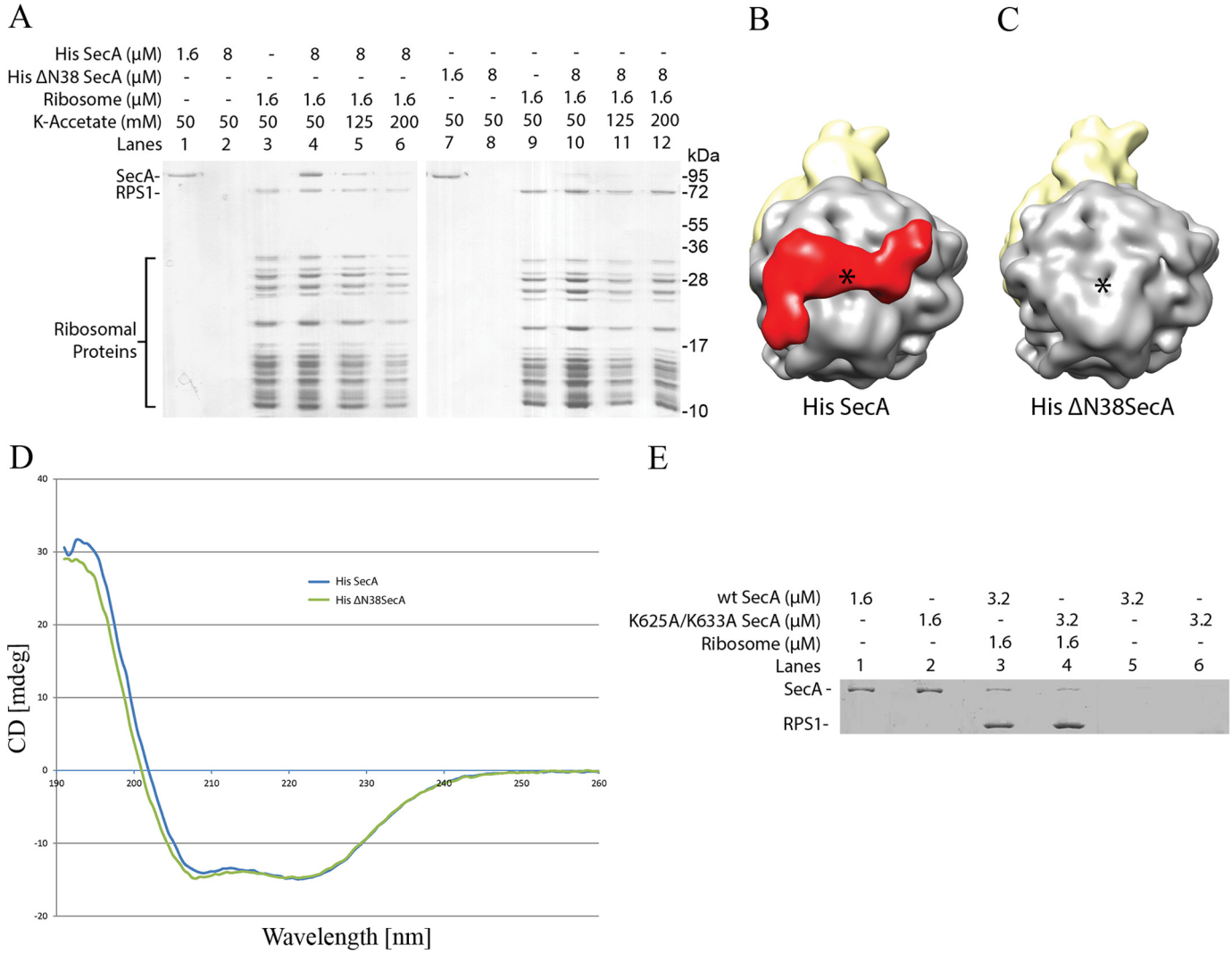

FIGURE 7. **The N-terminal helix of SecA is required for stable interactions with the ribosome.** *A*, deletion of residues 2–38 at the N terminus of SecA (Δ*N38 SecA*) severely reduces binding to the ribosome. The cosedimentation assay shows binding of full-length SecA to the 70S ribosome as before in Fig. 1 (*lane 4*), whereas binding is almost abolished with ΔN38 SecA (*lane 10*) under the same conditions. Binding of full-length SecA is salt-sensitive (*lanes 5–6*), as shown before in Fig. 1. *Lanes 3* and *9* contain 1.6 μM 70S ribosomes pelleted alone. Both of the SecA and ΔN38 SecA alone did not sediment (*lanes 2* and *8*). 1.6 μM each of the SecA and ΔN38 SecA proteins were applied on the gel as a control (*lanes 1* and *7*). *B*, low-resolution reconstruction of the 70S ribosome reconstituted with full-length SecA. Density in the *red* color at the tunnel exit site represents SecA bound in the 70S structure. The structure is reconstructed from SecA-bound particles (about 80%, 5500 particles) consisting of both the monomeric and dimeric forms, sorted from empty ribosomes (about 20%), and filtered between 20 and 25 Å. *C*, low-resolution reconstruction of the 70S ribosome reconstituted with ΔN38 SecA. No SecA density is visible in the structure. The structure is reconstructed from about 6000 particles without any sorting (because there was no SecA density visible in any of the reconstructions) and filtered between 20 and 25 Å. The color scheme is the same as before. The *asterisk* marks the polypeptide tunnel exit. *D*, CD spectra of SecA and ΔN38 SecA, as indicated. *E*, binding of K625A/K633A SecA to the ribosome. 1.6 μM purified 70S ribosomes were incubated with wild-type SecA (*lane 3*) or with SecA (K625A/K633A) (*lane 4*) as indicated. Binding reactions were pelleted through a sucrose cushion and analyzed on a 10% SDS-PAGE with Coomassie Blue staining. Both the wild-type and SecA (K625A/K633A) proteins alone did not sediment (*lanes 5* and *6*). 1.6 μM wild-type and (K625A/K633A) SecA proteins were applied on the gel as a control (*lanes 1* and *2*).

SecA. In one of the structures from *Bacillus subtilis* (PDB code 2IBM), the minimum distance between the α-helical linker domain and the N terminus of SecA is as small as 3.5 Å. Considering the close proximity of the N terminus of SecA to the helical linker domain, it is possible that replacing residues in this helical linker domain might affect the stability of the N terminus, resulting in a decrease in binding to the ribosome (as observed by Huber *et al.* (38 and by us).

Two SecA Binding Sites on the Ribosome—Our structures revealed two forms of SecA bound to the ribosome (Fig. 3), *i.e.* both the single copy (monomeric) as well as the double copies (dimeric). However, it is not clear whether SecA interacts with the ribosome first in a monomeric form, followed by recruitment of the second monomer, which then results in a dimer, or whether preformed SecA dimers bind to the ribosome. Because the oligomeric state of SecA is highly debated and conflicting evidence has been proposed about the functional state of SecA (3, 16–20), this aspect was investigated further. We reasoned that if monomeric SecA binds to the ribosome, disrupting dimer formation should not inhibit binding to the ribosome. This was investigated by two different approaches. First, we titrated SecA protein concentration into the reconstitution with 70S ribosomes because lowering the concentration would shift the equilibrium toward the monomeric form. Low-resolu-

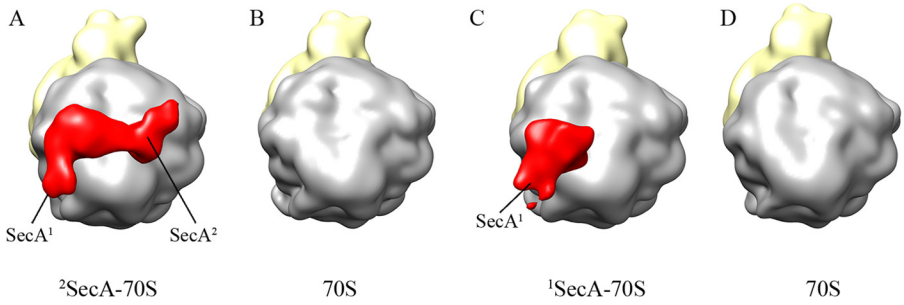

FIGURE 8. **SecA displays different affinities for the two binding sites on the ribosome.** Low-resolution structures of 70S ribosome reconstituted with SecA under different conditions. About 6000–8000 particles were used for the three-dimensional reconstruction using a non-translating 70S ribosome as a reference. Sorting was applied to segregate the SecA-bound 70S from unbound 70S using an empty 70S ribosome. Structures are filtered between 20 and 25 Å. *A*, 70S structure with SecA bound under the same conditions as before. The structure is reconstructed from SecA-bound particles (about 80%), consisting of both the monomeric and dimeric form sorted from empty ribosomes (about 20%). *B*, SecA was pretreated with 0.05% DDM before addition to 70S ribosomes in the same buffer as in *A*. The structure is reconstructed from about 6500 particles without any sorting because there was no SecA density visible in any of the reconstructions. *C*, SecA was incubated with 70S ribosomes as in *A*, and, after binding, 0.05% DDM was added to the reaction, followed by 5 min of incubation at room temperature before freezing the grids. The structure is reconstructed from SecA-bound particles (about 55%) consisting of mainly the monomeric form sorted from empty ribosomes (45%). *D*, the same as *C*, but DDM was increased from 0.05 to 0.10%. The structure is reconstructed from about 6500 particles without any sorting because there was no SecA density visible in any of the reconstructions. No binding was observed when SecA was pretreated with 0.05% DDM (*B*). When the same amount of DDM was added after binding of SecA, only one copy of SecA was observed (*C*), indicating dissociation and selective removal of one copy from the two copies of bound complex. The color scheme is the same as before.

tion structures were reconstructed to visualize 70S-bound SecA. Interestingly, lowering the SecA concentration to half (about a 9-fold molar excess) resulted in only monomeric SecA being visible in the structure (data not shown). Lowering the SecA concentration further resulted in no SecA density visible in the structure. This result indicates that the single copy of SecA (monomeric, $SecA^1$) can stably bind to the ribosome. Second, the detergent *n*-dodecyl-β-maltoside (DDM) was used to disrupt dimers of SecA, as shown previously (22). When SecA was pretreated with 0.05% DDM before reconstitution with the ribosome, low-resolution 70S reconstruction showed no density for SecA (Fig. 8*B*). This probably suggests that dissociation of SecA dimers into monomers results in loss of binding to the ribosome. However, when SecA was allowed to bind to the ribosome and 0.05% DDM was added only after binding, the density corresponding to the single copy of SecA (monomeric, $SecA^1$) was visible in the 70S structure (Fig. 8*C*). Further increasing the DDM concentration to 0.1% resulted in no SecA density being visible in the structure (Fig. 8*D*). These results further support the notion that SecA binds to the ribosome at two different sites formed by the ribosomal proteins L23 and L22/L24, respectively (Fig. 6). Additionally, these results indicate that the two binding sites present on the ribosome display different affinities for SecA (Fig. 6). However, this might change when a signal peptide is present. As observed by Huber *et al.* (38), SecA binds strongly to a ribosome translating the SecM nascent chain, a known substrate for SecA.

At the concentrations used in our experiments, SecA would mainly be present in a dimeric form, and so it is surprising to see a stable monomeric form of SecA ($SecA^1$) bound in our structure. Docking of the dimeric SecA models (PDB codes 2IBM, 2IPC, and 2FSF) in our ^{2}SecA structure resulted in only one of the two copies fitting in the density (supplemental Fig. S2). This suggests that SecA might initially interact with the ribosome as a dimer and that the binding to the ribosome leads to the dissociation of the second copy of SecA ($SecA^2$), which later reassociates to form a new elongated dimeric form present in our structure (^{2}SecA-70S). These results also suggest that the observed dimer interface/interaction formed between two SecA molecules, when bound to the ribosome in the ^{2}SecA-70S structure, is rather weak and represents an arrangement without any productive interaction. This could also explain why the dimeric interface in our structure (^{2}SecA) is different from the crystal structures of SecA.

Implications for SecA Binding to the Ribosome—Our study identified two SecA binding sites in the immediate vicinity to the ribosome tunnel exit. A first SecA monomer ($SecA^1$) binds to the ribosome through an interaction with the L23 protein, followed by binding of a second molecule ($SecA^2$) to the L22/L24 proteins, resulting in two copies of SecA bound to the ribosome (Figs. 4 and 6). Upon superimposition of the ribosome-bound cryo-EM model of trigger factor (TF) (50) with SecA, no steric clashes between monomeric SecA and TF were observed, although both bind to the L23 protein near the tunnel exit (Fig. 9*A*). This observation suggests that both the TF and monomeric SecA could possibly bind to the ribosome simultaneously without competition. However, this state would prevent binding of a second copy of SecA. In this case, both the monomeric SecA and TF can simultaneously scan for their respective substrates emerging from the tunnel exit. When a substrate has been recognized by monomeric SecA, it might lead to recruitment of the second copy of SecA at the tunnel exit by displacing TF. Interestingly, SRP also binds to the L23 protein (51, 52). Superimposing molecular models of SecA and SRP reveal a steric clash, suggesting competition between monomeric SecA and SRP for binding to the L23 protein (Fig. 9*B*). This suggests that monomeric SecA directly competes with SRP for binding to the ribosome and that either SecA or SRP can bind to the ribosome at any given time. Surprisingly, our *in vitro* binding assays showed a strong affinity of SecA toward the non-translating/empty ribosomes. This unusually high affinity is a result of the lack of competition from other factors such as SRP, SecYEG, and peptide deformylase (PDF) present inside the cell. In a recent report, Wu *et al.* (53) studied competitive binding of SecYEG to the ribosome and SecA. However, further studies are required to study the molecular interplay between SecA, the

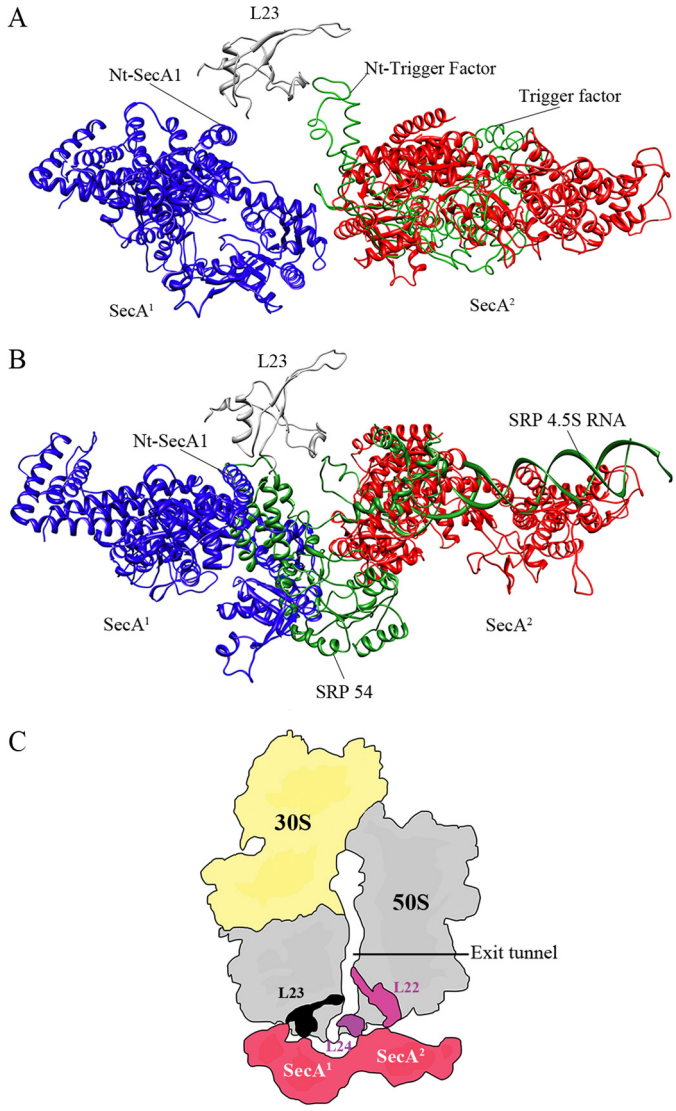

FIGURE 9. **Superimposition of the ^{2}SecA-70S, trigger factor, and signal recognition particle models.** *A*, both the TF and SecA^{1} could bind simultaneously to the ribosome via L23 protein without steric hindrance, although it would prevent binding of the second copy of SecA (SecA^{2}) to the ribosome. SecA^{1} is colored in *blue*, SecA^{2} in *red*, TF in *green*, and L23 in *gray*. *B*, binding of both the SecA^{1} and SRP to the ribosome could cause steric hindrance, thus suggesting competition between monomeric SecA and SRP for binding to the L23 protein. Only either SecA or SRP can bind to the ribosome at any given time. SRP is colored in *green*, and SecA and L23 are shown as in *A*. *C*, schematic of SecA binding to the ribosome. The first molecule interacts with the ribosome via the L23 protein, whereas the second one interacts with L22/L24 proteins at the polypeptide tunnel exit. Two copies of SecA completely surround the tunnel exit and might provide a unique environment for the incoming nascent polypeptides. The color scheme is the same as before, except that the L23 protein is shown in *black*.

ribosome, and the SecYEG translocase during protein sorting and translocation in the presence of other targeting and processing factors such as SRP, TF, PDF, and methionine aminopeptidase (49).

In conclusion, we show that not only a SecA monomer binds to the ribosome but, also, that two copies of SecA can be observed in an elongated shape. Two copies of SecA completely surround the tunnel exit and might provide a unique environment to nascent secretory preproteins emerging form the ribosomal tunnel (Fig. 9*C*). Our structures suggest a possible function of the dimeric form of SecA at the ribosome and will provide a framework for further research in the protein sorting and translocation field.

Acknowledgments—We thank K. Heinze, H. Schindelin, and A. Ludwig for critical reading of the manuscript and B. Sander for help with CD spectroscopy.

REFERENCES

1. Park, E., and Rapoport, T. A. (2011) Mechanisms of Sec61/SecY-mediated protein translocation across membranes. *Annu. Rev. Biophys.* **41,** 21–40
2. Lycklama, A., Nijeholt, J. A., and Driessen, A. J. (2012) The bacterial Sec-translocase. Structure and mechanism. *Philos. Trans. R. Soc. Lond. B. Biol. Sci.* **367,** 1016–1028
3. Akita, M., Shinkai, A., Matsuyama, S., and Mizushima, S. (1991) SecA, an essential component of the secretory machinery of *Escherichia coli*, exists as homodimer. *Biochem. Biophys. Res. Commun.* **174,** 211–216
4. Rollo, E. E., and Oliver, D. B. (1988) Regulation of the *Escherichia coli* secA gene by protein secretion defects. Analysis of secA, secB, secD, and secY mutants. *J. Bacteriol.* **170,** 3281–3282
5. Hunt, J. F., Weinkauf, S., Henry, L., Fak, J. J., McNicholas, P., Oliver, D. B., and Deisenhofer, J. (2002) Nucleotide control of interdomain interactions in the conformational reaction cycle of SecA. *Science* **297,** 2018–2026
6. Vassylyev, D. G., Mori, H., Vassylyeva, M. N., Tsukazaki, T., Kimura, Y., Tahirov, T. H., and Ito, K. (2006) Crystal structure of the translocation ATPase SecA from *Thermus thermophilus* reveals a parallel, head-to-head dimer. *J. Mol. Biol.* **364,** 248–258
7. Zimmer, J., Li, W., and Rapoport, T. A. (2006) A novel dimer interface and conformational changes revealed by an X-ray structure of *B. subtilis* SecA. *J. Mol. Biol.* **364,** 259–265
8. Osborne, A. R., Clemons, W. M., Jr., and Rapoport, T. A. (2004) A large conformational change of the translocation ATPase SecA. *Proc. Natl. Acad. Sci. U.S.A.* **101,** 10937–10942
9. Papanikolau, Y., Papadovasilaki, M., Ravelli, R. B., McCarthy, A. A., Cusack, S., Economou, A., and Petratos, K. (2007) Structure of dimeric SecA, the *Escherichia coli* preprotein translocase motor. *J. Mol. Biol.* **366,** 1545–1557
10. Zimmer, J., Nam, Y., and Rapoport, T. A. (2008) Structure of a complex of the ATPase SecA and the protein-translocation channel. *Nature* **455,** 936–943
11. Erlandson, K. J., Miller, S. B., Nam, Y., Osborne, A. R., Zimmer, J., and Rapoport, T. A. (2008) A role for the two-helix finger of the SecA ATPase in protein translocation. *Nature* **455,** 984–987
12. Gelis, I., Bonvin, A. M., Keramisanou, D., Koukaki, M., Gouridis, G., Karamanou, S., Economou, A., and Kalodimos, C. G. (2007) Structural basis for signal-sequence recognition by the translocase motor SecA as determined by NMR. *Cell* **131,** 756–769
13. Musial-Siwek, M., Rusch, S. L., and Kendall, D. A. (2007) Selective photoaffinity labeling identifies the signal peptide binding domain on SecA. *J. Mol. Biol.* **365,** 637–648
14. Papanikou, E., Karamanou, S., Baud, C., Frank, M., Sianidis, G., Keramisanou, D., Kalodimos, C. G., Kuhn, A., and Economou, A. (2005) Identification of the preprotein binding domain of SecA. *J. Biol. Chem.* **280,** 43209–43217
15. Kusters, I., van den Bogaart, G., Kedrov, A., Krasnikov, V., Fulyani, F., Poolman, B., and Driessen, A. J. (2011) Quaternary structure of SecA in solution and bound to SecYEG probed at the single molecule level. *Structure* **19,** 430–439
16. Driessen, A. J. (1993) SecA, the peripheral subunit of the *Escherichia coli* precursor protein translocase, is functional as a dimer. *Biochemistry* **32,** 13190–13197
17. Woodbury, R. L., Hardy, S. J., and Randall, L. L. (2002) Complex behavior in solution of homodimeric SecA. *Protein Sci.* **11,** 875–882
18. Sardis, M. F., and Economou, A. (2010) SecA. A tale of two protomers. *Mol. Microbiol.* **76,** 1070–1081
19. Jilaveanu, L. B., Zito, C. R., and Oliver, D. (2005) Dimeric SecA is essential

for protein translocation. *Proc. Natl. Acad. Sci. U.S.A.* **102,** 7511–7516
20. Jilaveanu, L. B., and Oliver, D. (2006) SecA dimer cross-linked at its subunit interface is functional for protein translocation. *J. Bacteriol.* **188,** 335–338
21. Benach, J., Chou, Y. T., Fak, J. J., Itkin, A., Nicolae, D. D., Smith, P. C., Wittrock, G., Floyd, D. L., Golsaz, C. M., Gierasch, L. M., and Hunt, J. F. (2003) Phospholipid-induced monomerization and signal-peptide-induced oligomerization of SecA. *J. Biol. Chem.* **278,** 3628–3638
22. Or, E., Navon, A., and Rapoport, T. (2002) Dissociation of the dimeric SecA ATPase during protein translocation across the bacterial membrane. *EMBO J.* **21,** 4470–4479
23. Musial-Siwek, M., Rusch, S. L., and Kendall, D. A. (2005) Probing the affinity of SecA for signal peptide in different environments. *Biochemistry* **44,** 13987–13996
24. de Keyzer, J., van der Sluis, E. O., Spelbrink, R. E., Nijstad, N., de Kruijff, B., Nouwen, N., van der Does, C., and Driessen, A. J. (2005) Covalently dimerized SecA is functional in protein translocation. *J. Biol. Chem.* **280,** 35255–35260
25. Randall, L. L., Crane, J. M., Lilly, A. A., Liu, G., Mao, C., Patel, C. N., and Hardy, S. J. (2005) Asymmetric binding between SecA and SecB two symmetric proteins. Implications for function in export. *J. Mol. Biol.* **348,** 479–489
26. Karamanou, S., Sianidis, G., Gouridis, G., Pozidis, C., Papanikolau, Y., Papanikou, E., and Economou, A. (2005) *Escherichia coli* SecA truncated at its termini is functional and dimeric. *FEBS Lett.* **579,** 1267–1271
27. Whitehouse, S., Gold, V. A., Robson, A., Allen, W. J., Sessions, R. B., and Collinson, I. (2012) Mobility of the SecA 2-helix-finger is not essential for polypeptide translocation via the SecYEG complex. *J. Cell Biol.* **199,** 919–929
28. Morita, K., Tokuda, H., and Nishiyama, K. (2012) Multiple SecA molecules drive protein translocation across a single translocon with SecG inversion. *J. Biol. Chem.* **287,** 455–464
29. Das, S., and Oliver, D. B. (2011) Mapping of the SecA. SecY and SecA. SecG interfaces by site-directed *in vivo* photocross-linking. *J. Biol. Chem.* **286,** 12371–12380
30. Deville, K., Gold, V. A., Robson, A., Whitehouse, S., Sessions, R. B., Baldwin, S. A., Radford, S. E., and Collinson, I. (2011) The oligomeric state and arrangement of the active bacterial translocon. *J. Biol. Chem.* **286,** 4659–4669
31. Osborne, A. R., and Rapoport, T. A. (2007) Protein translocation is mediated by oligomers of the SecY complex with one SecY copy forming the channel. *Cell* **129,** 97–110
32. Tsukazaki, T., Mori, H., Fukai, S., Ishitani, R., Mori, T., Dohmae, N., Perederina, A., Sugita, Y., Vassylyev, D. G., Ito, K., and Nureki, O. (2008) Conformational transition of Sec machinery inferred from bacterial SecYE structures. *Nature* **455,** 988–991
33. Tziatzios, C., Schubert, D., Lotz, M., Gundogan, D., Betz, H., Schägger, H., Haase, W., Duong, F., and Collinson, I. (2004) The bacterial protein-translocation complex. SecYEG dimers associate with one or two SecA molecules. *J. Mol. Biol.* **340,** 513–524
34. Hsieh, Y. H., Zhang, H., Lin, B. R., Cui, N., Na, B., Yang, H., Jiang, C., Sui, S. F., and Tai, P. C. (2011) SecA alone can promote protein translocation and ion channel activity. SecYEG increases efficiency and signal peptide specificity. *J. Biol. Chem.* **286,** 44702–44709
35. Hsieh, Y. H., Zhang, H., Wang, H., Yang, H., Jiang, C., Sui, S. F., and Tai, P. C. (2013) Reconstitution of functionally efficient SecA-dependent protein-conducting channels. Transformation of low-affinity SecA-liposome channels to high-affinity SecA-SecYEG-SecDF. YajC channels. *Biochem. Biophys. Res. Commun.* **431,** 388–392
36. Lin, B. R., Hsieh, Y. H., Jiang, C., and Tai, P. C. (2012) *Escherichia coli* membranes depleted of SecYEG elicit SecA-dependent ion-channel activity but lose signal peptide specificity. *J. Membr. Biol.* **245,** 747–757
37. Karamyshev, A. L., and Johnson, A. E. (2005) Selective SecA association with signal sequences in ribosome-bound nascent chains. A potential role for SecA in ribosome targeting to the bacterial membrane. *J. Biol. Chem.* **280,** 37930–37940
38. Huber, D., Rajagopalan, N., Preissler, S., Rocco, M. A., Merz, F., Kramer, G., and Bukau, B. (2011) SecA interacts with ribosomes to facilitate post-translational translocation in bacteria. *Mol. Cell* **41,** 343–353
39. Clemons, W. M., Jr., Brodersen, D. E., McCutcheon, J. P., May, J. L., Carter, A. P., Morgan-Warren, R. J., Wimberly, B. T., and Ramakrishnan, V. (2001) Crystal structure of the 30 S ribosomal subunit from *Thermus thermophilus*. Purification, crystallization and structure determination. *J. Mol. Biol.* **310,** 827–843
40. Kitagawa, M., Ara, T., Arifuzzaman, M., Ioka-Nakamichi, T., Inamoto, E., Toyonaga, H., and Mori, H. (2005) Complete set of ORF clones of *Escherichia coli* ASKA library (a complete set of *E. coli* K-12 ORF archive). Unique resources for biological research. *DNA Res.* **12,** 291–299
41. Bhushan, S., Hoffmann, T., Seidelt, B., Frauenfeld, J., Mielke, T., Berninghausen, O., Wilson, D. N., and Beckmann, R. (2011) SecM-stalled ribosomes adopt an altered geometry at the peptidyl transferase center. *PLoS Biol.* **9,** e1000581
42. Mindell, J. A., and Grigorieff, N. (2003) Accurate determination of local defocus and specimen tilt in electron microscopy. *J. Struct. Biol.* **142,** 334–347
43. Frank, J., Radermacher, M., Penczek, P., Zhu, J., Li, Y., Ladjadj, M., and Leith, A. (1996) SPIDER and WEB. Processing and visualization of images in 3D electron microscopy and related fields. *J. Struct. Biol.* **116,** 190–199
44. Penczek, P. A., Frank, J., and Spahn, C. M. (2006) A method of focused classification, based on the bootstrap 3D variance analysis, and its application to EF-G-dependent translocation. *J. Struct. Biol.* **154,** 184–194
45. Emsley, P., and Cowtan, K. (2004) Coot. Model-building tools for molecular graphics. *Acta Crystallogr. D Biol. Crystallogr.* **60,** 2126–2132
46. Pettersen, E. F., Goddard, T. D., Huang, C. C., Couch, G. S., Greenblatt, D. M., Meng, E. C., and Ferrin, T. E. (2004) UCSF Chimera. A visualization system for exploratory research and analysis. *J. Comput. Chem.* **25,** 1605–1612
47. Kiefer, F., Arnold, K., Künzli, M., Bordoli, L., and Schwede, T. (2009) The SWISS-MODEL Repository and associated resources. *Nucleic Acids Res.* **37,** D387–392
48. Seidelt, B., Innis, C. A., Wilson, D. N., Gartmann, M., Armache, J. P., Villa, E., Trabuco, L. G., Becker, T., Mielke, T., Schulten, K., Steitz, T. A., and Beckmann, R. (2009) Structural insight into nascent polypeptide chain-mediated translational stalling. *Science* **326,** 1412–1415
49. Kramer, G., Boehringer, D., Ban, N., and Bukau, B. (2009) The ribosome as a platform for co-translational processing, folding and targeting of newly synthesized proteins. *Nat. Struct. Mol. Biol.* **16,** 589–597
50. Merz, F., Boehringer, D., Schaffitzel, C., Preissler, S., Hoffmann, A., Maier, T., Rutkowska, A., Lozza, J., Ban, N., Bukau, B., and Deuerling, E. (2008) Molecular mechanism and structure of Trigger Factor bound to the translating ribosome. *EMBO J.* **27,** 1622–1632
51. Halic, M., Blau, M., Becker, T., Mielke, T., Pool, M. R., Wild, K., Sinning, I., and Beckmann, R. (2006) Following the signal sequence from ribosomal tunnel exit to signal recognition particle. *Nature* **444,** 507–511
52. Schaffitzel, C., Oswald, M., Berger, I., Ishikawa, T., Abrahams, J. P., Koerten, H. K., Koning, R. I., and Ban, N. (2006) Structure of the *E. coli* signal recognition particle bound to a translating ribosome. *Nature* **444,** 503–506
53. Wu, Z. C., de Keyzer, J., Kedrov, A., and Driessen, A. J. (2012) Competitive binding of the SecA ATPase and ribosomes to the SecYEG translocon. *J. Biol. Chem.* **287,** 7885–7895